Available online at www.sciencedirect.com
SCIENCE DIRECT®
C. R. Chimie 8 (2005) 597–607
COMPTES RENDUS CHIMIE
http://france.elsevier.com/direct/CRAS2C/

Account / Revue

Organized mesoporous solids: mechanism of formation and use as host materials to prepare carbon and oxide replicas

Bénédicte Lebeau [a,*], Julien Parmentier [a], Michel Soulard [a], Christobel Fowler [a], Raoul Zana [b], Cathie Vix-Guterl [c], Joël Patarin [a]

[a] *Laboratoire de matériaux minéraux, CNRS UMR 7016, ENSCMu, université de haute Alsace, 3, rue Alfred-Werner, 68093 Mulhouse cedex, France*
[b] *Institut Charles-Sadron, CNRS UPR 22, université Louis-Pasteur, 6, rue Boussingault, 67000 Strasbourg, France*
[c] *Institut de chimie des surfaces et interfaces, CNRS UPR9069, ENSCMu, université de haute Alsace, 15, rue Jean-Starcky, 68087 Mulhouse cedex, France*

Received 21 July 2004; accepted after revision 1 October 2004

Available online 26 January 2005

Abstract

Since the discovery of organized mesoporous solids by Mobil Oil Co. scientists, numerous patents and papers dealing with the synthesis, mechanism of formation, properties and applications of these exciting solids have been published. In this context, our research group has focused its activities on two research area: (*i*) the understanding of the formation of silica and alumina mesostructured solids using in situ probing techniques such as fluorescence, and (*ii*) the development of new synthesis routes such as nanocasting, with the aim of preparing ordered mesoporous carbons and oxides with tailored properties. This short review reports the main results that we have obtained in recent years on these topics. ***To cite this article: B. Lebeau et al., C. R. Chimie 8 (2005).***

Résumé

Depuis la découverte des solides mésoporeux organisés par des chercheurs de la Mobil Oil Co., de nombreux brevets et publications concernant la synthèse, les mécanismes de formation, les propriétés et les applications de ces solides innovants ont été publiés. Dans ce contexte, notre groupe de recherche a focalisé ses activités selon deux axes : (*i*) la compréhension de la formation de silice et d'alumine mésostructurées, en utilisant des techniques de sondage in situ telles que la fluorescence, et (*ii*) le développement de nouvelles voies de synthèse comme le nanomoulage, dans le but de préparer des carbones et des oxydes mésoporeux ordonnés et à propriétés spécifiques. Cette courte revue présente les principaux résultats obtenus au cours de ces dernières années par notre équipe. ***Pour citer cet article : B. Lebeau et al., C. R. Chimie 8 (2005).***

* Corresponding author.
E-mail address: benedicte.lebeau@uha.fr (B. Lebeau).

1631-0748/$ - see front matter © 2004 Académie des sciences. Published by Elsevier SAS. All rights reserved.
doi:10.1016/j.crci.2004.10.001

Keywords: Ordered mesoporous solids; Mechanism of formation; Fluorescence techniques; Nanocasting; Carbon replicas; Oxide replicas

Mots clés : Solides mésoporeux organisés ; Mécanisme de formation ; Techniques de fluorescence ; Nanomoulage ; Répliques carbone ; Répliques oxyde

1. Introduction

In the 1990s, the synthesis of a new family of organized mesoporous silica molecular sieves, prepared in the presence of surfactants and designated as M41S, opened a new field of research in materials science [1]. Ordered mesoporous silicas (OMS) represent a wide range of structures with diverse symmetry, pore size, pore shape and pore connectivity. Nowadays, the preparation of these materials can generally be well-controlled due to the high stability of silica under numerous conditions, and the fact that mesoscopic organizations rely on the use of surfactants as directing agents or surfactant micelles or liquid crystals as organic templates. These materials have high potential in many applications, particularly in the fields of supported catalysis, separation processes, and host-guest chemistry. These applications could be widely extended with the development of non-siliceous oxide analogues in area such as catalysis and photocatalysis for example [2]. However, non-siliceous ordered porous oxides are less common and do not offer a similarly large variety of structures. This is related to the difficulty, in controlling the self organic–inorganic assembly process. Moreover, removal of the organic template after synthesis generally leads to the formation of dense phases. Therefore, two approaches have been developed in our research group to tackle these problems: (i) the elucidation of the mechanisms of formation of such ordered mesoporous solids (siliceous and non-siliceous oxides) and (ii) the development of new preparation routes to overcome these synthesis drawbacks.

This brief review provides a summary of the key results obtained in our group through the use of these two approaches.

2. Study of the mechanisms of formation of mesostructured oxide-based solids

Fluorescence probing techniques can provide extremely important information regarding the mechanism of formation of mesostructured materials. Recall that fluorescent probing techniques probe systems in situ, and can be applied to the study of clear solutions (called precursor systems in this article). Such techniques have been demonstrated to be highly effective, as they enable one to determine the size and the shape of (*the*) surfactant micelles, and to characterize their environment [3,4]. Time-resolved fluorescence quenching is the method of choice. Indeed, the micellar form and size are deduced from measurements of the micelle aggregation number, N, which represents the number of surfactants (*molecules*) per micelle. Additionally, the exchange of two counterions at the micelle surface can be characterized by fluorescence lifetime measurements if one of the ions is a quencher of the probe fluorescence. We have applied these techniques to study the mechanism of formation of mesostructured hexagonal silica and alumina MCM-41 type materials prepared in the presence of cetyltrimethylammonium bromide (CTAB) or chloride (CTAC) and sodium dodecylsulfate (SDS) as surfactants, respectively. Two different probe molecules, pyrene and dipyrenylpropane, were used in time-resolved fluorescence quenching and fluorescence emission experiments; cetylpiridinium chloride being introduced as a quencher of the pyrene fluorescence. From these fluorescence studies, the following parameters can be obtained: (i) micelle micropolarity and micro viscosity from the emission spectra of pyrene (I_1/I_3 intensity ratio) and dipyrenylpropane ($I_{\mathrm{Monomer}}/I_{\mathrm{Excimer}}$ intensity ratio), respectively, (ii) micelle aggregation number (N) and pyrene fluorescence lifetime (τ) from the fluorescence decay curves of micelle-solubilized pyrene.

2.1. Ordered mesoporous silica

Several of the mechanisms previously proposed for the formation of the MCM-41-type solids postulate an ion exchange in solution between the silicate species and the surfactant counterions at the micelle surface [5,6]. They suggest accumulation of silicate ions around

the micelles (template), prior to the micelle growth and condensation of the inorganic species, as a key step. The ion exchange would be a driving force for micelle elongation into rod-like arrangements that leads to the liquid crystalline (LC) silica phase.

We have used the fluorescence techniques (spectrofluorometry and time-resolved fluorescence quenching), as described above, for studying the silicate/counterion exchanges taking place at the micelle surface [3]. This study yielded information on the changes in the properties of the micelles under the synthesis conditions leading to the formation of MCM-41 materials. Fluorescence measurements were performed on highly alkaline CTAB- or CTAC-sodium silicate solutions (pH 13.6) and before silica polymerization (pH 11.6).

The precursor systems (clear solutions) used for preparing the MCM-41-type materials had the following composition: 0.5 M SiO_2 (water glass or $(Si_8O_{20})^{8-}$ species (also called D4R units)) + 0.1 M CTAB or CTAC + 0.9–1.0 M NaOH and/or TMAOH. Additional experiments were performed at higher surfactant concentrations, up to 0.5 M. The pH of the systems was decreased from 13.5 to 11.6 by dropwise addition of concentrated HCl, or by replacing part of the NaOH by NaCl in precursor systems. This second method enabled us to avoid the precipitation of a small amount of material upon addition of concentrated HCl to the system at pH < 12, even under extensive stirring. The various reference systems required for this study are listed in Table 1.

Under the experimental conditions used in this investigation, i.e. using homogeneous precursor systems prior to precipitation, the results obtained from in situ fluorescence probing showed that; (*i*) for CTAB-containing systems, micelle-bound bromide ions, (well-known for quenching the pyrene fluorescence), were exchanged only to a small extent by the added hydroxyl ions or silicate species (only a very small increase of the pyrene fluorescence life time was observed), (*ii*) very little growth of the CTAB or CTAC micelles could be detected in the presence of silicate ions (the aggregation number N remained nearly constant), (*iii*) micellar growth was small as the pH was lowered to a value just above that where a solid precipitated out, and (*iv*) no organic mesophase was present prior to precipitation.

A possible mechanism for the formation of OMS consistent with the above observations was proposed (see Fig. 1). State **A** represents the initial CTA^+X^- ($X = Br^-$ or Cl^-) aqueous solution which contains spherical micelles ($N_{CTAB} = 145$; $N_{CTAC} = 101$; $\tau_{CTAB} = 165$ ns; $\tau_{CTAC} = 342$ ns, see Table 1) in equilibrium with free surfactant ions and free counterions. For the sake of clarity, only one micelle is represented, with about 80% of the micellized surfactant ions neu-

Table 1
Deaerated precursor systems CTAB/SiO_2/NaOH, CTAC/SiO_2/NaOH and CTAB/SiO_2/TMAOH: values of the pyrene intensity ratio I_1/I_3 (micropolarity); $\tau_E I_M/I_E$ (microviscosity); pyrene fluorescence lifetime (τ); micelle aggregation number (N); and fraction of exchanged micelle-bound bromide ions f^{Br}_{exch}

System composition	I_1/I_3	$\tau_E I_M/I_E$ (ns)	τ (ns)	f^{Br}_{exch}	N
Systems with water glass as silica source					
0.1 M CTAB	1.35	572	165	0	145
0.1 M CTAB + 0.5 M NaOH	1.35	569	177	0.13	149
0.1 M CTAB + 0.5 M SiO_2 + 0.9 M NaOH	1.35	650	180	0.16	161
0.3 M CTAB			158	0	
0.3 M CTAB + 0.5 M NaOH			161	0.04	
0.3 M CTAB + 0.645 M NaOH + 0.5 M SiO_2			159	0.02	
0.5 M CTAB			151.5	0	
0.5 M CTAB + 0.645 M NaOH + 0.5 M SiO_2			155	0.04	
0.1 M CTAC			342		101
0.1 M CTAC + 0.5 M SiO_2 + 0.9 M NaOH			342		116
0.5 M CTAC			342		125
0.5 M CTAC + 1.0 M NaOH + 0.5 M SiO_2			328		155
Systems with D4R as silica source					
0.1 M CTAB; 21% (v/v) MeOH			195		81
0.1 M CTAB + 1.0 M TMAOH			196		127
0.1 M CTAB + 1.0 M TMAOH; 21% (v/v) MeOH			247		77
0.1 M CTAB + 0.5 M SiO_2 + 1.0 M TMAOH; 21% (v/v) MeOH			272		96

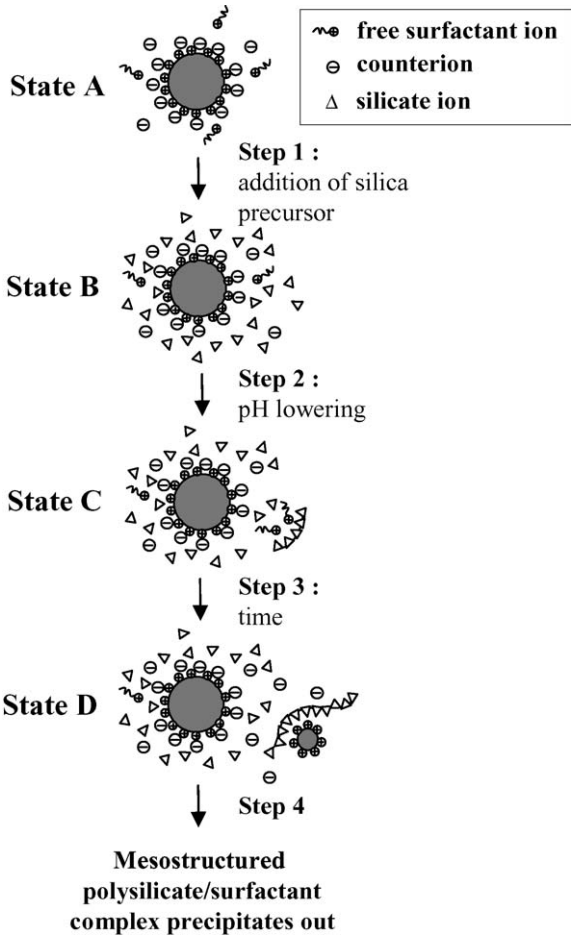

Fig. 1. Scheme of the mechanism of formation of the mesostructured silica synthesized by lowering the pH of a highly alkaline CTAB-sodium silicate solution (adapted from Ref. [3]).

tralized by bound counterions [7]. Step **1** consists of the addition of highly alkaline silicate species to the system. A small fraction of micelle-bound bromide ions are exchanged by OH^- or silicate ions as represented by state **B** (τ_{CTAB} = 180 ns; τ_{CTAC} = 342 ns), where the micelle has one bound silicate ion, but most bound counterions are still bromide ions. In step **2** the pH is lowered and the system may be also heated, as described in the literature [1,8]. The effect of these external factors is to initiate the polymerization of silicate species. The formation of silica prepolymers with low degree of polymerization (DP) follows, as represented in state **C** of the system. These prepolymers are assumed to be negatively charged, as precipitation starts at a pH well above the isoelectric point of silica. The prepolymers may start binding a few surfactant ions. Such behavior would be consistent with reports that show that in systems consisting of polyelectrolytes and oppositely charged surfactant ions, the number of bound surfactant ions and the cooperativity of the binding increase rapidly with the DP of the polyelectrolyte [9,10]. At this stage, a model similar to that proposed by Huo et al. [11] can explain the formation of the organic-inorganic mesostructured material. After some time has elapsed following pH lowering (step **3**), the silicate prepolymers have grown further and can now bind more surfactant in a more cooperative manner. At this stage we have micelle-like polymer-bound aggregates. This corresponds to state **D** in Fig. 1. During step **3** and subsequent steps, the micelles simply act as reservoirs of surfactant ions, supplying the ions that bind to the growing silicate polymers. Extensive binding of the prepolymers to the CTAB micelles before precipitation does not occur. This would be accompanied by a release of counterions, and would thus give rise to a significant increase in the pyrene lifetime, contrary to what is observed. Such binding cannot be excluded with CTAC, as chloride ions are bound less strongly than bromide ions and are thus more easily exchanged with oligosilicate ions. However, as inferred above, the accumulation of silicate ions at the micelle surface is not an important feature in the formation of OMS. State **D** corresponds to the system just before precipitation of a silicate polymer/surfactant complex, as illustrated in step **4**. Indeed, precipitation of a polyelectrolyte/surfactant complex has been found to occur in all polyelectrolyte/oppositely charged surfactant systems [12,13].

Our model focuses on the existence of electrostatic (charge–charge) interactions between negatively charged silica polymers and free surfactant cations, and not on micelles and added silicate species. In this model, the surfactant micelles act as surfactant reservoirs. It supports the ideas put forward by Göltner and Antonietti [14] who indeed stated that "the precipitation (of an organized material) is comparable to that of polyelectrolyte/surfactant complexes." The geometry of the resulting material is controlled by charge density matching at the organic-inorganic interface.

2.2. Ordered mesostructured alumina (OMA)

The mechanism of formation of mesostructured or mesoporous alumina has not been extensively studied

in the past. We focused our study on a hexagonally mesostructured alumina precipitated in the presence of SDS and urea, as reported by Yada et al. [15]. Under these conditions, the increase in pH was obtained by the slow decomposition of urea at 60 °C. The materials obtained at a final pH of between 6 and 7 all exhibit the same characteristics. They display three XRD peaks between $2\theta = 1$ and 10°, which can be clearly indexed to hexagonal symmetry, with (100), (110) and (200) indexes. This mesostructure can be confirmed using transmission electron microscopy, where images show a honeycomb network. The MCM-41 type materials possess a worm-like morphology [16].

The system described above is particularly well adapted for a study of the mechanisms of formation of organized mesostructured aluminas. Indeed, the slow decomposition of urea allows a progressive increase in pH. The species organize slowly and can be observed in situ in the clear precursor solution.

Our investigations mainly involved the reference systems 0.60 M SDS and 0.60 M SDS/9.1 M urea, and the precursor system 0.60 M SDS/9.1 M urea/0.30 M $Al(NO_3)_3$, at a temperature of 60 °C. Firstly, the micelle aggregation number, the micelle microviscosity, and the pyrene fluorescence lifetime were determined for the initial state of these systems (i.e. before the onset of polymerization). The effects of substitution of $Al(NO_3)_3$ by $AlCl_3$ or $NaNO_3$ and of a change in the concentrations of SDS and $Al(NO_3)_3$ were also investigated. The micelles present in the precursor system were found to have an aggregation number of 105, which indicates a slightly elongated shape, and an ionization degree around 0.12, indicating strong binding of Al^{3+} ions to the micelle surface. The bound Al^{3+} ions were shown to carry a small amount of nitrate ions to the micelle surface, to the extent of about 5 mol% with respect to SDS. The bound nitrate ions strongly quenched the pyrene fluorescence. Similar results were obtained for the dilute precursor system 0.10 M SDS/9.1 M urea/0.30 M $Al(NO_3)_3$ and for the corresponding reference systems. In a second step the systems were studied as a function of the aging time (time spent at 60 °C). The microviscosity of the micelles in the precursor system increased with the aging time. This result, together with the variation in the time after which a precipitate was observed in the system with the SDS concentration strongly supports a mechanism where the main locus for polymerization is the micelle surface.

Three facts suggest that the polymerization most likely occurs at the micelle surface. First, the concentration of Al^{3+} ions at the micelle surface is much larger than that in the bulk phase. Secondly, the micelle microviscosity increases with the aging time. Thirdly, the time required for precipitation of the mesostructured alumina increases with the SDS concentration. A scheme of the mechanism proposed for the formation of the mesostructured alumina is given in Fig. 2. In a 0.6 mol l^{-1} aqueous solution of SDS at 60 °C (state **A**), N is equal to 74, value which corresponds to quasi-spherical micelles, and τ is equal to 310 ns. When urea is added to the previous solution (step **1**), so as to have a urea concentration of 9.1 mol l^{-1} (state **B**), N and τ decrease to 53 and 280 ns, respectively. A direct mecha-

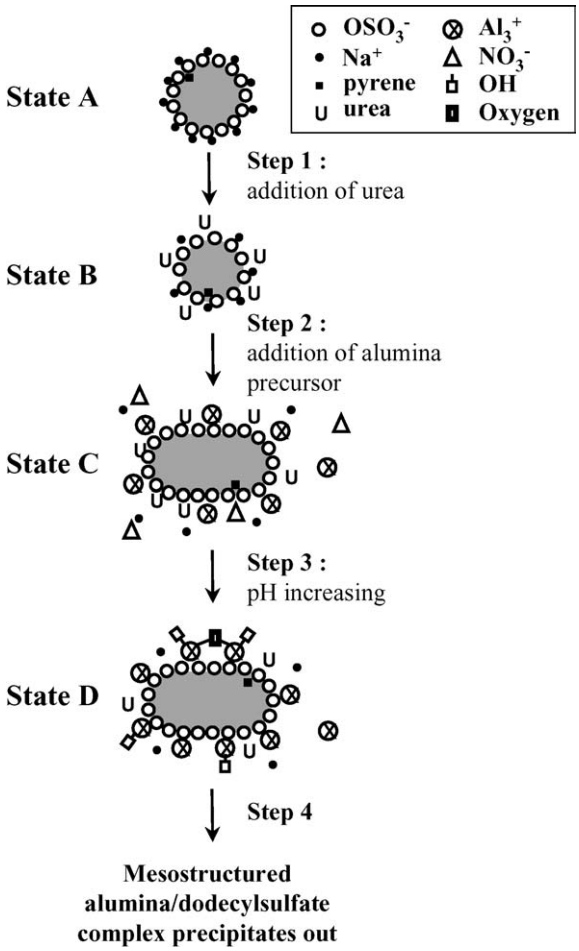

Fig. 2. Scheme of the mechanism of formation of the mesostructured alumina synthesized in the presence of sodium dodecyl sulfate and urea (adapted from Ref. [4]).

nism which involves the penetration of urea molecules in the micelle palisade layer can explain these results [17]. Finally, the addition of aluminum nitrate (step **2**) at a concentration of 0.3 mol l^{-1} to the SDS/urea system leads to the precursor solution (state **C**) used to synthesize the mesostructured alumina. In this precursor system in the initial state **C** (t = 0 h), the dodecylsulfate micelles are surrounded by bound aluminum cations, some urea molecules, and a few nitrate anions, responsible for the quenching of the pyrene fluorescence. The decomposition of urea is accompanied by the formation of hydroxyl ions, and the pH increases gradually from 3.5 at time zero to 5.5 at the end of the process. The increase in the pH (step **3**) initiates the formation of charged complex oxygenated aluminum species that can begin polymerizing (state **D**). The growing polymeric species remain completely or partially bound to the negatively charged micelles via electrostatic interactions between their residual positive charge and the negatively charged sulfate head groups at the micelle surface. On the contrary, the initially bound nitrate ions progressively leave the micelles because the positive charge per aluminum bound on the polymer decreases as polymerization proceeds. This brings about the observed increase in the pyrene fluorescence lifetime. The growing inorganic polymers may bind several micelles, and micelle cross-linking by inorganic polymers may occur. Nevertheless, both light scattering and time-resolved fluorescence studies indicate that most of the growth of the inorganic polymer and of the polymer/surfactant micelle complexes takes place shortly before precipitation occurs. The complexes precipitate out once they become sufficiently large. Their organization into a mesostructured hexagonal material occurs during or very shortly before precipitation. It is likely that this precipitation event involves a near complete neutralization of the micelle charge by the residual charge on the polymers. Indeed, the material that precipitates out does not contain sodium and nitrate ions. In this case, contrary to what is observed for the silica-based system discussed above [3], the growing polymeric species remain completely or partially bound to the negatively charged micelles at the start of the process. This occurs via electrostatic interactions between their residual positive charge and the negatively charged sulfate head groups at the micelle surface. However, the complex organization into a mesostructured hexagonal material occurs during or shortly before precipitation.

The mechanisms presented in this review are adequately supported by the experimental data described above and others [18,19]. It is clear that the interaction between the inorganic precursor and the template is the key factor in the control of the material mesostructure. However, the step where such interactions occur is still open to debate, and appears to depend strongly on the synthesis conditions used. One must bear in mind that none of these mechanisms provides an exclusive or definitive answer. Indeed, the characterization techniques are limited in terms of sampling and experimental time scale for example. Moreover, they probe only one part of the system, while the formation of these materials involves numerous steps. These steps can be separated in three main stages: liquid (precursor solution), solid/liquid (precipitate) and solid state (final material). This complexity probably explains the differences observed between the mechanisms proposed in the literature. In situ synchrotron small angle X-ray scattering study of the formation of mesoporous silica [20] appear capable of bringing new information on the unsettled issues.

3. Synthesis of ordered mesoporous carbon and oxide materials via nanocasting, using OMS as host matrices

3.1. The nanoduplication process

An organized mesoporous material exhibiting three-dimensional porosity (MCM-48, SBA-15 for example) is used as a mould with a non-siliceous oxide or carbon precursor. After treatment of the precursor, the mould is selectively removed using an appropriate chemical treatment, and a negative oxide or carbon replica material is obtained. This process is particularly interesting in the preparation of materials such as carbons, for which porosity has traditionally been difficult to tailor using conventional means [21]. Moreover, these templated carbons can be considered to be model materials, possessing well-controlled pore sizes and pore distributions. Such materials are of prime interest for the enhanced understanding of the textural parameters which need to be optimized in the design of high performance supercapacitors and hydrogen storage carbon materials.

We have therefore, investigated the influence of various experimental conditions (host material, carbon pre-

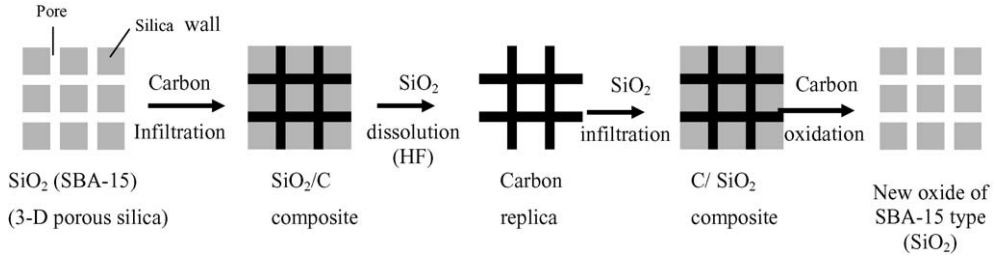

Fig. 3. Schematic representation of the nanocasting process used for the preparation of carbon and oxide (silica) replicas.

cursor, and degree of infiltration) on the physico-chemical properties of the carbon materials synthesized. The preparation of an oxide replica (silica) has also been performed, starting from a carbon host material obtained by nanocasting, subsequently infiltrated with a silica precursor. The carbon was removed by oxidation. A schematic representation of the nanocasting process used in this work is presented in Fig. 3.

3.2. Preparation of the carbon replicas

The nanocasting process allows for control of the preparation of tailored carbon materials. A wide choice of experimental parameters (template, infiltration procedure, secondary treatments for example) determine the physico-chemical properties of the carbon replicas, such as the microporosity/mesoporosity ratio, surface area, total pore volume, pore features and graphitization state. Various parameters concerned with the template can also be controlled. For example pore diameter, wall thickness (which corresponds to porosity within the replica) and pore morphology and connectivity. Nevertheless, a 3-D porous network is required for cohesion of the replica. The properties of the replicas can also be greatly influenced by the infiltration procedure, which is determined by the choice of the carbon precursor, the degree of infiltration, and the temperature of conversion into carbon. In this review, we focus on the influence of the carbon precursor on the properties of the carbon replica obtained from an SBA-15 template (1-D mesopores arranged in a honneycomb structure and interconnected by micropores) and infiltrated with a similar carbon content (close to 35 wt.%). The sucrose and pitch carbon precursors were infiltrated via a liquid procedure, while the propylene was infiltrated via a gaseous procedure.

The *sucrose process* was performed as reported by Ryoo et al. [22] and is not described in detail here. Briefly, a liquid solution of sucrose was mixed with the silica host matrix at room temperature in the presence of a H_2SO_4 catalyst, before drying and subsequently impregnation with a second sucrose solution. The mixture was then heat-treated in a vacuum at 1173 K for 3 h. These two liquid-impregnation steps allow a carbon content of 36 wt.% to be reached for the SiO_2/C material.

The *chemical vapor deposition* (*CVD*) *process* is based on the pyrolytic decomposition of propylene (2.5 vol.% in Argon) at 1023 K on the porous silica matrix, as reported elsewhere [23,24]. The duration of the deposition allows a control of the carbon content in the final SiO_2/C material. Values in the range 22–52 wt.% of carbon into the SiO_2/C composite material have been obtained, compared with the maximal theoretical value of approximately 63 wt.% which could be infiltrated in the SBA-15 host material (considering a pore volume of 1.0 cm^3 g^{-1} and a silica and carbon density of 2.2 and 1.8, respectively).

For the *Pitch process*, petroleum pitch named 'Ashland A240' was used as the carbon precursor [25]. A calculated amount of pitch (density of 1.24) was mixed with the silica template in order to fill all of the mesopores. The pitch impregnation was performed by stirring this mixture for 4 h at 575 K (temperature corresponding to the lowest viscosity of the pitch). The silica/Pitch mixture was cooled down before being heat-treated in argon up to 1175 K (heating rate: 3 K min^{-1}) for the conversion of pitch to carbon. With a pitch having a carbon yield of 45 wt.%, a carbon content of about 36 wt.% was obtained for the SiO_2/C sample after one impregnation. Moreover, pitch is an excellent source of graphitizable carbon, [26,27] since the calcined mesophase formed during the pitch carbonization generates a pre-graphitic structure that can be developed into a graphitic structure by high-temperature treatment.

3.3. Characterization of the carbon replicas (according to the preparation procedure)

The carbon replicas have been characterized by XRD, SEM, TEM and N_2 adsorption–desorption isotherms [24,25]. The comparison of the isotherms of the carbon materials reported in Fig. 4 reveals different porous features according to the precursor used. The microporous character can be attributed to the intrinsic nature of the carbon that depends on the precursor. The mesoporous characteristic is determined by the manner the precursor infiltrates into the host matrix. Indeed, although the porosity of a carbon replica should correspond strictly to that released after the silica walls dissolution, an additional porosity exists which is related to the voids existing in the SiO_2/C materials. This peculiar porosity depends (i) on the amount of carbon infiltrated (e.g. with 35 wt.% of C present in the SiO_2/C composite, 70% of the starting silica pore volume remains unfilled) and (ii) on the nature of the carbon precursor which could lead to inhomogeneous pore filling or even pore blocking. Moreover, according to the precursor and its associated process, different cell parameter contractions are observed (Table 2) for the carbon replicas that influence their pore volumes. For instance, for low relative pressures (below 0.05), a high nitrogen uptake is observed for the carbon deriving from the sucrose precursor ($C_{sucrose}$); it corresponds to a material presenting a high surface area (Table 2) with presumably a microporous character created by the gas release that occurs during the carbonization of sucrose

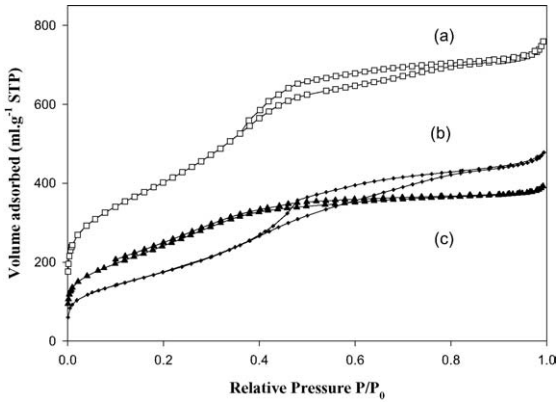

Fig. 4. Nitrogen adsorption/desorption isotherms at 77 K of the SBA-15 carbon replicas, from the sucrose precursor (a), from the propylene precursor (b), from the pitch precursor (c), with a carbon amount infiltrated close to 35 wt.%.

Table 2
Some characteristics of SBA-15 carbon replicas

Sample	V_p ($cm^3\ g^{-1}$)	S_{BET} ($m^2\ g^{-1}$)	Variation of the unit cell compared to the silica SBA-15 (%)[a]
$C_{CVD-35\%}$	0.7	650	6
$C_{Sucrose-35\%}$	1.1	1500	16
$C_{Pitch\ 1-35\%}$	0.6	920	8

V_p: total pore volume; S_{BET}: specific surface area.
[a] For the SBA-15 silica matrix, the hexagonal unit-cell parameter is equal to 11.2 nm.

[28]. For higher relative pressures, the porosity observed from the isotherms corresponds to the space created by the silica wall removal. A high nitrogen adsorption value again indicates a high mesoporous character for the material. However, the large pore volume (1.1 $cm^3\ g^{-1}$) of this carbon replica is quite surprising if one considers that this sample had the highest cell parameter shrinkage (16% relative to the silica template) (Table 2). It is believed that the strong contraction of the precursor that occurs during the carbonization is not totally accommodated by the silica matrix. Thus, voids in-between the SiO_2 and C may appear. This additional porosity is then released by the silica dissolution and contributes to the total pore volume. The $C_{Propylene}$ sample presents a similar isotherm shape but with less marked mesoporous character. The carbon material arising from pitch (C_{Pitch}) exhibits no hysteresis, and must therefore possess mesopores of smaller diameter. A typical XRD pattern of a carbon replica is shown in Fig. 5.

Complementary studies (not reported here) using other silica moulds have confirmed that the porosity

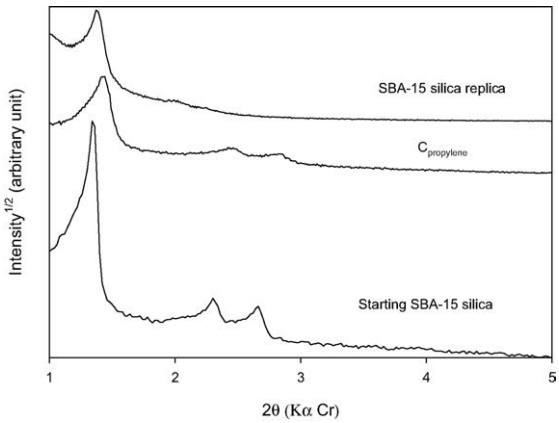

Fig. 5. XRD patterns of the starting SBA-15 silica and the resulting carbon and silica replicas (adapted from Ref. [29]).

can be controlled by the choice of the template. Nevertheless, this work revealed that the carbon precursor and amount of carbon infiltrated into the host matrix are key parameters for the control of the porous characteristics of the carbon replica. Moreover, the precursor determines the intrinsic properties of the carbon, such as its composition and its ability to graphitize.

3.4. Study of the influence of the infiltration process onto the silica template

The physico-chemical properties of ordered mesoporous carbons obtained by this negative replication process are strongly influenced by their method of preparation. In order to get a better understanding of the carbon formation, the structural evolution of a mesoporous silica template before and after C infiltration with propylene and sucrose (and a subsequent oxidation), was studied using various techniques such as XRD, N_2 adsorption/desorption and TEM [28]. The MCM-48 silica material was chosen as a template because of its hydrothermal sensitivity related to its thin walls (approximately 1 nm), and its highly regular structure. It was shown that the use of a liquid carbon precursor such as a sucrose solution led to a strong alteration in the silica template (decrease in the symmetry, loss of long-range ordering, and disappearance of the narrow mesopore size distribution). This was attributed to (*i*) the high-temperature of the process (1173 K) and (*ii*) the water vapor released during the carbonization that hydrolyzed the poorly hydrothermally stable silica network. On the contrary, the pyrolytic decomposition of a gaseous carbon precursor such as propylene, performed at a lower temperature (1023 K) and without water release, only led to minor modifications. These behaviors may influence the physico-chemical properties of the resulting carbon. For both impregnation processes, carbon acts as a highly stable porogenic agent. Heat-treatment at a temperature as high as 1473 K in an inert atmosphere, and subsequent oxidation to remove the carbon, succeeded in preserving the long-range order and surface area of the starting silica template. To the contrary, under similar experimental conditions and in the absence of carbon, a complete loss of organization at the mesoscopic scale was observed.

3.5. Applications of the carbon replicas

The possibility to synthesize well tailored nanostructured carbon materials is of prime importance for predicting the optimal porous characteristics of an electrode material used in capacitor applications. For instance, the highly ordered structure of MCM-48 mesoporous silica materials infiltrated with sucrose precursors allows one to prepare interesting carbon materials with potential applications as electrode materials for supercapacitors [29,30] or hydrogen storage [31]. This is due, in the former case, to its original and unique interconnected porous structure and high surface area, along with a well balanced micro/mesoporosity that allows a quick charge propagation of the ions to the active surface. Good characteristics with capacitance values as high as 200 and 110 F g^{-1} have been obtained in aqueous and organic media, respectively.

3.6. Preparation of new oxide (SiO_2) by nanocasting

In order to investigate the strategy for the synthesis of the new oxide illustrated in Fig. 3, the preparation of an OMS using impregnation of silica into a SBA-15 type carbon replica was investigated. The latter was infiltrated by a gaseous silica precursor (tetraethylorthosilicate (TEOS)) using a gas-phase process [32], and the carbon was successively removed by oxidation. It is worthy to note that liquid infiltration processes using sodium silicate solution [33] or TEOS [34] as silica liquid precursor, were also successfully used for the preparation of such silica replicas.

The XRD patterns of the starting SBA-15 silica, its carbon replica and the resulting silica replica are shown in Fig. 5. One can clearly see (as confirmed by TEM) that the hexagonal structure is maintained for the three materials. A minor discrepancy observed is a cell parameter contraction (shift of the XRD peaks towards higher two theta angle values), for the carbon and silica replicas. Such behavior may be explained by the low amount of incorporated silica, along with its shrinkage during the various heat-treatments (1223 K in argon and 973 K in air for the oxidation of the carbon). A decrease in the peak intensity is also clear, which is consistent with a partial loss of the long-range organization after repeated replications.

The two silica materials (parent and replica) were also characterized by nitrogen adsorption/desorption

measurements and their isotherms are reported in Fig. 6. The starting SBA-15 silica exhibits a type IV isotherm with a characteristic steep step at P/P_0 close to 0.7 for the adsorption branch indicating a narrow pore size distribution of large pores. The use of the BJH model gave a pore diameter of 5.5 nm. The inverse silica replica obtained from the SBA-15 type carbon template exhibits, as expected, isotherms similar to those of the SBA-15 material, with a P/P_0 step of approximately 0.7. This corresponds, according to the BJH model, to a pore diameter of 6.0 nm. Compared to the starting silica material, the pore size is slightly larger; and could be related to the two successive and incomplete carbon and silica fillings that were performed for the preparation of the silica replica. The corresponding pore volume and surface area are around 550 $m^2\ g^{-1}$ and 1.0 $cm^3\ g^{-1}$, respectively. The use of the chemical vapor infiltration technique with TEOS as gaseous silica precursor to duplicate a mesoporous silica has been demonstrated, with the advantage that a relatively uniform replica can be obtained, with regard to structure, symmetry, pore size and pore volume, with only minor loss of organization. It is reasonable to assume that this gaseous nanoduplication process (which occurs via a carbon template) can be extended to numerous oxides such as alumina, titania, and zirconia for example. Indeed, the CVI of oxides has already proven to be suitable for filling porosity with various oxides [35]. Moreover, the extensive choice of OMS templates should allow for the formation of a vast number of non-siliceous mesoporous materials using this technique.

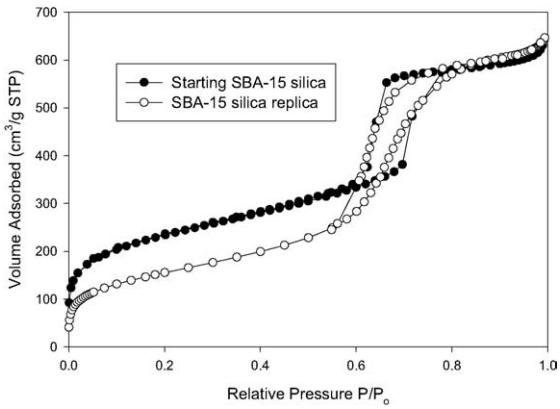

Fig. 6. Nitrogen adsorption/desorption isotherms at 77 K of the starting SBA-15 silica and the resulting silica replica (adapted from Ref. [29]).

4. Conclusion

In the first approach, the formation of silica and alumina-based MCM-41 type materials has been investigated by fluorescence probing techniques. These techniques permitted us to follow the changes of micelle micropolarity, microviscosity and aggregation number when generating step by step the systems that give rise to the mesotructured material either by lowering of the pH for silica or by heating in the presence of urea for alumina. It was also possible to know whether the ion exchange postulated in the templating mechanism really occurs. In the case of silica-based materials the results show that the CTAB micelles retain their bromide counterions and that only a few silicate anions come close to the micelle surface. In the case of alumina, the aluminum ions are indeed at the micelle surface. Nevertheless in both cases the results suggest that the formation of the mesostructured materials starts in the bulk phase. Interactions between the growing polymeric silica or alumina species and free surfactant ions in the intermicellar solution are the primary step in the formation of the mesotructured material. When the size of this polymer/surfactant complex becomes large enough it precipitates out and organizes. Complex nucleation/crystallization processes are involved at that stage.

The second approach that studies the formation and the properties of carbon and oxide replicas using a hard 'exotemplate' was also investigated. Starting from an organized mesoporous silica host matrix, various carbon replicas were prepared with physico-chemical properties such as pore morphology and size, surface area, composition, nanometric scale organization (graphitization).... determined by the silica template but also by the infiltration process and therefore by the choice of the carbon precursor. For instance, for a same carbon loading and a similar template, nanostructured carbons with surface areas ranging from 650 to 1500 $m^2\ g^{-1}$ could be obtained with the use of different precursors. These model carbon materials, with various controlled properties, contribute to determine their optimal specificities for some of their potential applications. Moreover, with the development of the nanocasting process, these carbon materials also open a new research field for the formation of non-siliceous oxide and ceramic nanoporous replicas.

Acknowledgments

The authors would like to thank Dr. J. Dentzer for discussion and the PhD students involved in this work: J. Frasch, L. Sicard, S. Saadhallah and M. Reda. Financial supports from the French Ministry of Research ('Action concertée incitative Nanosciences et Nanotechnologies 2002' (project:NN060); 'Action concertée energie 2003' (Pr1-2)) and the 'Centre national de la recherche scientifique' (CNRS) (&OpenCurlyQuot'Programme Matériaux 2002' – project No. 41 and C.E. Fowlers grant) are also gratefully acknowledged.

References

[1] C.T. Kresge, M.E. Leoniwicz, W.J. Roth, J.C. Vartuli, J.S. Beck, Nature 359 (1992) 710.
[2] F. Schüth, Chem. Mater. 13 (2001) 3184.
[3] J. Frasch, B. Lebeau, M. Soulard, J. Patarin, R. Zana, Langmuir 16 (2000) 9049.
[4] L. Sicard, B. Lebeau, J. Patarin, R. Zana, Langmuir 18 (2002) 74.
[5] A. Firouzi, D. Kumar, L.M. Bull, T. Besier, P. Sieger, Q. Huo, S.A. Lker, J.A. Zasadzinski, C. Glinka, J. Nicol, D. Margolese, G.D. Stucky, B.F. Chmelka, Science 267 (1995) 1138.
[6] A. Galarneau, F. Di Renzo, F. Fajula, L. Mollo, B. Fubini, M.F. Ottaviani, J. Colloid Interf. Sci. 201 (1998) 105.
[7] R. Zana, J. Colloid Interf. Sci. 78 (1980) 330.
[8] J.S. Beck, J.C. Vartuli, W.J. Roth, M.E. Leonowicz, C.T. Kresge, K.D. Schmitt, et al., J. Am. Chem. Soc. 114 (1992) 10834.
[9] J. Liu, N. Takisawa, K. Shirahama, H. Abe, K. Sakamoto, J. Phys. Chem. B 101 (1997) 7520.
[10] J. Liu, K. Shirahama, T. Miyajima, J.C.T. Kwak, Colloid Polym. Sci. 276 (1998) 40.
[11] Q. Huo, D. Margolese, U. Ciesla, D.G. Demuth, P. Feng, T.E. Gier, P. Sieger, A. Firouzi, B.F. Chmelka, F. Schüth, G.D. Stucky, Chem. Mater. 6 (1994) 1176.
[12] E.D. Goddard, Colloids Surf. 19 (1986) 301.
[13] See for instance: J.C.T. Kwak (Ed.), Polymer–Surfactant Systems, Marcel Dekker, Inc., New York, 1998
[14] C. Göltner, M. Antonietti, Adv. Mater. 9 (1997) 431.
[15] M. Yada, H. Hiyoshi, K. Ohe, M. Machida, T. Kalima, Inorg. Chem. 36 (1997) 5565.
[16] L. Sicard, P.L. Llewellyn, J. Patarin, F. Kolenda, Micropor. Mesopor. Mater. 44 (45) (2001) 195.
[17] C.C. Ruiz, Colloids Surf. A 147 (1999) 349.
[18] A. Caragheorgheopol, H. Caldarary, M. Vasilescu, A. Khan, D. Angelescu, N. Zilkova, J. Cejka, J. Phys. Chem. B 106 (2004) 7735.
[19] F. Né, F. Testard, T. Zemb, I. Grillo, Langmuir 19 (2003) 8503.
[20] K. Flodström, C.V. Texeira, H. Amenitisch, V. Alfredsson, M. Linden, Langmuir 20 (2004) 4885.
[21] T. Kyotani, Carbon 38 (2000) 269.
[22] R. Ryoo, S.H. Joo, S. Jun, J. Phys. Chem. B 103 (1999) 7743.
[23] J. Parmentier, J. Patarin, J. Dentzer, C. Vix-Guterl, Ceram. Int. 28 (2002) 1.
[24] C. Vix-Guterl, S. Boulard, J. Parmentier, J. Werckmann, J. Patarin, Chem. Lett 10 (2002) 1062.
[25] C. Vix-Guterl, S. Saadhallah, L. Vidal, M. Reda, J. Parmentier, J. Patarin, J. Mater. Chem. 13 (2003) 2535.
[26] I. Mochida, Y. Korai, C. Ku, F. Watanabe, Y. Sakai, Carbon 38 (2000) 305.
[27] B. Rand, Design and Control of Structure of Advanced Carbon Materials for Enhanced Performance, Kluwer Academic Publishers, The Netherlands, 2001, p. 135.
[28] J. Parmentier, C. Vix-Guterl, P. Gibot, M. Reda, M. Ilescu, J. Werckmann, J. Patarin, Micropor. Mesopor. Mater. 62 (2003) 87.
[29] C. Vix-Guterl, S. Saadallah, E. Frackowiak, K. Jurewicz, M. Reda, J. Parmentier, J. Patarin, F. Béguin, Mater. Sci. Eng. B 108 (2004) 148.
[30] K. Jurewicz, C. Vix-Guterl, E. Frackowiak, S. Saadhallah, M. Reda, J. Parmentier, J. Patarin, F. Béguin, J. Phys. Chem. Solids 65 (2004) 287–293.
[31] R. Gadiou, S. Saadallah, T. Piquerot, P. David, J. Parmentier, C. Vix-Guterl, Micropor. Mesopor. Mater. 79 (2005) 121.
[32] J. Parmentier, C. Vix-Guterl, S. Saadallah, M. Reda, M. Illescu, J. Werckmann, J. Patarin, Chem. Lett. 32 (2003) 262.
[33] M. Kang, S.H. Yi, H.I. Lee, J.E. Yie, J.M. Kim, Chem. Commun. 17 (2002) 1944.
[34] A.-H. Lu, W. Schmidt, A. Taguchi, B. Spliethoff, B. Tesche, F. Schüth, Angew. Chem. Int. Ed. Engl. 41 (18) (2002) 3489.
[35] H.Y. Ha, S.W. Nam, T.H. Lim, H. Oh, S. Hong, J. Membr. Sci. 111 (1996) 81.